Atmos. Chem. Phys. Discuss., doi:10.5194/acp-2015-1020, 2016
Manuscript under review for journal Atmos. Chem. Phys.
Published: 18 January 2016

Atmospheric Chemistry and Physics Discussions

Biogenic cloud nuclei in the Amazon

J. D. Whitehead[1], E. Darbyshire[1], J. Brito[2], H. M. J. Barbosa[2], I. Crawford[1], R. Stern[3], M. W. Gallagher[1], P. H. Kaye[4], J. D. Allan[1], H. Coe[1], P. Artaxo[2], and G. McFiggans[1]

[1]Centre for Atmospheric Science, SEAES, University of Manchester, Oxford Road, Manchester, M13 9PL, UK
[2]Institute of Physics, University of São Paulo, Rua do Matão, Travessa R, 187. CEP 05508-090, São Paulo, S.P., Brazil
[3]Instituto Nacional de Pesquisas da Amazônia, Av. André Araújo, 2936, Aleixo, CEP 69060-001, Manaus, AM, Brazil
[4]Science and Technology Research Institute, University of Hertfordshire, AL10 9AB, UK

Correspondence to: G. McFiggans
(g.mcfiggans@manchester.ac.uk)

Abstract. The Amazon basin is a vast continental area in which atmospheric composition is relatively unaffected by anthropogenic aerosol particles. Understanding the properties of the natural biogenic aerosol particles over the Amazon rainforest is key to understanding their influence on regional and global climate. While there have been a number of studies during the wet season, and of biomass burning particles in the dry season, there has been relatively little work on the transition period - the start of the dry season in the absence of biomass burning. As part of the Brazil-UK Network for Investigation of Amazonian Atmospheric Composition and Impacts on Climate (BUNIAACIC) project, aerosol measurements, focussing on unpolluted biogenic air masses, were conducted above the canopy at a remote rainforest site in the Amazon, during the transition from wet to dry seasons, in July, 2013. This period marks the start of the dry season, but before significant biomass burning occurs in the region.

Median particle number concentrations were 266 cm^{-3}, with size distributions dominated by an accumulation mode of 130 - 150 nm. During periods of low particle counts, a smaller Aitken mode could also be seen around 80 nm. While the concentrations were similar in magnitude to those seen during the wet season, the size distributions suggest an enhancement in the accumulation mode compared to the wet season, but not yet to the extent seen later in the dry season, when significant biomass burning takes place. Submicron non-refractory aerosol composition, as measured by an Aerosol Chemical Speciation Monitor (ACSM), was dominated by organic material (86%).

Aerosol hygroscopicity was probed using measurements from a Hygroscopicity Tandem Differential Mobility Analyser (HTDMA), and a quasi-monodisperse Cloud Condensation Nuclei counter (CCNc). The hygroscopicity parameter, κ, was found to be low, ranging from 0.12 for Aitken mode particles to 0.18 for accumulation mode particles. This was consistent with previous studies in the region, but lower than similar measurements conducted in Borneo, where κ ranged 0.17 - 0.37, possibly due to a stronger marine influence at that location, bringing higher sulphate loadings than are typically seen in the Amazon.

A Wide Issue Bioaerosol Sensor (WIBS-3M) was deployed at ground level to probe the coarse mode, detecting primary biological aerosol by fluorescence (Fluorescent Biological Aerosol Particles, or FBAP). The mean FBAP number concentration was 404 $\pm$ 237 l^{-1}, however this was subject to a strong diurnal cycle, and ranged from around 200 l^{-1} during the day to as

Atmos. Chem. Phys. Discuss., doi:10.5194/acp-2015-1020, 2016
Manuscript under review for journal Atmos. Chem. Phys.
Published: 18 January 2016

Atmospheric Chemistry and Physics Discussions

much as 1200 l^{-1} at night. FBAP dominated the coarse mode particles, comprising more than 90% of particles detected by the WIBS-3 during the night. This proportion was also subject to a diurnal cycle, dropping to between 55% and 75% during the day, since non-FBAP did not show a strong diurnal pattern. Comparison with previous FBAP measurements above canopy at the same location suggests there is a strong vertical gradient in FBAP concentrations through the canopy. Application of Ward linkage cluster analysis using the z-score normalisation to the data suggests that FBAP were dominated (around 70%) by fungal spores. Further, long-term measurements will be required in order to fully examine the seasonal variability, and distribution through the canopy of primary biological aerosol particles.

This is the first time that such a suite of measurements has been deployed at this site to investigate the chemical composition and properties of the biogenic contributions to Amazonian aerosol during the transition period from the wet to dry seasons, and thus provides a unique contrast to the aerosol properties observed during the wet season in previous, similar campaigns. This was also the first deployment of a WIBS in the Amazon rainforest to study coarse mode particles, particularly primary biological aerosol particles, which is likely to play an important role as ice nuclei in the region.

1 Introduction

The Amazon Basin consists of the world's largest rainforest, covering an area of 5.5 million square kilometres. The Amazon rainforest is one of the few continental regions where atmospheric processes are minimally influenced by anthropogenic emissions, particularly during the wet season, and ambient conditions can represent, to some extent, those of the pristine pre-industrial era (Pöschl et al., 2010). Concentrations and properties of aerosol particles are largely governed by biogenic emissions, of both primary biological aerosol particles (PBAP) and biogenic volatile organic compounds (BVOC), which contribute to secondary organic aerosol (SOA). On a regional scale, in the wet season, the hydrological cycle is strongly influenced by these biogenic aerosol emissions, which provide most of the cloud condensation nuclei and thereby influence the radiation balance and cloud lifetime (Pöschl et al., 2010). In the dry season, by contrast, widespread biomass burning can result in a substantially increased aerosol optical depth over large areas of Amazonia, as well as modified cloud properties and suppressed precipitation (Andreae et al., 2004).

Previous studies in the pristine Amazon rainforest showed that fine particles (which account for most of the cloud condensation nuclei), consist mostly of secondary organic material derived from oxidised biogenic gases (Pöschl et al., 2010; Martin et al., 2010a; Allan et al., 2014; Chen et al., 2015). A lack of evidence for new particle formation during ground-based measurements (Zhou et al., 2002; Rissler et al., 2004; Martin et al., 2010a) implies that nucleation processes occur at higher altitudes, and new particles are entrained into the boundary layer from aloft (Krejci et al., 2005; Martin et al., 2010b). Larger super-micron particles are dominated by primary biological aerosol particles (PBAP) released from rainforest biota (Elbert et al., 2007; Pöschl et al., 2010; Huffman et al., 2012), which can play a significant role as ice nuclei (Prenni et al., 2009). These PBAP consist of wind-driven particles, such as pollen, bacteria, and plant debris, as well as actively ejected material, such as fungal and plant spores. Non-biological particles observed in the Amazon in the super-micron size range largely consist of advected Saharan dust and sea-salt from the Atlantic (Formenti et al., 2001; Worobiec et al., 2007; Martin et al., 2010b).

Atmos. Chem. Phys. Discuss., doi:10.5194/acp-2015-1020, 2016
Manuscript under review for journal Atmos. Chem. Phys.
Published: 18 January 2016

Atmospheric Chemistry and Physics Discussions

The low aerosol number concentrations in the pristine Amazon rainforest (typically a few hundred cm^{-3}) mean that CCN activation in convective clouds is often aerosol limited (Pöschl et al., 2010). It is clear that there is a strong coupling between the rainforest biosphere and the hydrological cycle in the Amazon Basin, with biogenic aerosol particles providing the nuclei for clouds, which in turn sustain the rainforest through precipitation (Pöschl et al., 2010).

Improving our knowledge of these processes is necessary to understanding the influence the Amazon rainforest has on regional and global climate and atmospheric composition, and how changing land use and climate in Amazonia will impact on this (Artaxo et al., 2013). To this end, the Brazil-UK Network for Investigation of Amazonian Atmospheric Composition and Impacts on Climate (BUNIAACIC) was established to define and nurture a framework within which future UK contributions to studies in these areas may be coordinated. As part of the BUNIAACIC project, a short-term intensive measurement campaign was undertaken at a pristine rainforest site in July, 2013, focusing on aerosol particle concentrations and properties during clean, pollution-free conditions. The timing permitted a study of the natural aerosol at the start of the dry season, which could be compared to previous measurements made during the wet season. Here we present the results of this study.

2 Methodology

2.1 Measurement Site and Sampling

The measurements were conducted at a remote site in pristine Amazonian rainforest between the 4th and 28th July 2013, during the transition from the wet to dry seasons. This is around the start of the dry season, but before significant biomass burning takes place. In July 2013, the total rainfall measured was 153 mm, mostly concentrated at the start and end of the month (during the measurement period itself, the rainfall was 77 mm). For the purposes of comparison, the AMAZE-08 campaign (Martin et al., 2010a) saw 370 mm fall over the course of 5 weeks during the wet season. Conditions were also cooler and more humid than during the current study.

Sampling was done at the TT34 tower (2°35'40"S 60°12'33"W, elevation 110 m), in the Reserva Biológica do Cuieiras, approximately 60 km NNW of the city of Manaus in Brazil. The site is representative of near-pristine conditions, and no biomass burning takes place within the reservation, however the site can be affected by regional transport of pollutants including emissions from Manaus and biomass burning (Artaxo et al., 2013; Rizzo et al., 2013). Locally, accommodation for researchers and a 60 kW diesel generator were situated 0.33 km and 0.72 km, respectively, in a WNW direction from the tower. Intensive measurement campaigns have taken place at this site in the past (e.g. Martin et al., 2010a), and long term measurements have been conducted since 2008 (Artaxo et al., 2013; Rizzo et al., 2013). During this experiment, local time was UTC - 4 hours.

A laminar sample flow of about 17 lpm was drawn through a 3/4" OD stainless steel line from a height of 39 m (about 10 m above canopy height) down to a ground level air conditioned container, in which the instruments were housed. Before entering the container, the sample was passed through an automatic regenerating adsorption aerosol dryer (Tuch et al., 2009). This kept the RH in the sample flow to between 20% and 40%. Instruments drawing off this dried sample flow included a Hygroscopicity Tandem Differential Mobility Analyser (HTDMA; University of Manchester), and a Cloud Condensation Nuclei counter (CCNc; CCN-100, Droplet Measurement Technologies). Upstream of these instruments, the sample flow (2

Atmos. Chem. Phys. Discuss., doi:10.5194/acp-2015-1020, 2016
Manuscript under review for journal Atmos. Chem. Phys.
Published: 18 January 2016

Atmospheric Chemistry and Physics Discussions

lpm) was further dried to an RH of between 15% and 25% with a nafion dryer operating with a counterflow of dry compressed air. The flow then passed through an electrical ionizer (model 1090, MSP Corporation), providing a charge-neutralised aerosol sample to the instruments. These same instruments were deployed in Borneo during the OP3 project (Irwin et al., 2011). Further details of the HTDMA and CCNc are given below.

Core instruments running at the site, on the same inlet, included a Multi Angle Absorption Photometer (MAAP; model 5012, Thermo-Scientific), a Condensation Particle Counter (CPC; model 3772, TSI), and an Aerosol Chemical Speciation Monitor (ACSM; Aerodyne Research Inc.). The ACSM was used to measure mass concentrations of particulate ammonium, nitrate, sulphate, chloride, and organic species in the submicron size range. Mass calibration was obtained by sampling mono disperse ammonium nitrate and ammonium sulphate. Further instrumental details and data post-processing is given by Brito et al. (2014). A weather station (Davis, USA) at the top of the tower provided meteorological data (wind speed and direction, temperature, RH, etc.).

As well as the instruments in the container, a Wide Issue Bioaerosol Sensor (WIBS; model 3M, University of Hertfordshire) was operated in a weatherproof box on the ground, a short distance from the base of the tower, with a short (1 m) 1/4" OD stainless steel inlet (more details are provided below). Other core instruments running at the site, but not used in this study, are detailed by Artaxo et al. (2013).

2.2 HTDMA measurements

In the HTDMA (Cubison et al., 2005; Good et al., 2010), a dry aerosol sample is size-selected with the first DMA and then humidified to a set RH. The second DMA is then used to measure the size distribution of the humidified aerosol, to give the distribution of Growth Factor (defined as the ratio of humidified to dry aerosol diameter: D/D_0) as a function of RH and dry diameter (GF_{RH,D_0}). Quality assurance and inversion of the data was performed using the TDMAinv toolkit of Gysel et al. (2009). During normal operation, the first DMA cycled through 5 dry sizes (45 nm, 69 nm, 102 nm, 154 nm and 269 nm; calibrated values), and the monodisperse flow after the first DMA was humidified to a target RH of 90%. The RH measured in DMA2 remained fairly stable ($\pm$2%) for most of the measurement period, and the variation was accounted for by correcting the data to the target RH within the inversion toolkit (Gysel et al., 2009). In addition to this normal mode of operation, humidograms were run on the 21st and 23rd July. In this mode, cycling through 3 dry sizes (45 nm, 102 nm and 269 nm), the RH in the second DMA was gradually varied between 45% and 95% in order to determine how the GF of ambient aerosol varies with RH.

In both DMAs, a ratio of 10:1 was maintained between the sheath and sample flows, and these were calibrated using a bubble flowmeter (Gillibrator, Sensidyne). The first DMA was size calibrated at the start of measurements using NIST-traceable latex spheres (Fisher Scientific), nebulised with an aerosol generator (model ATM 226; TOPAS). Dry scans (in which the sample is not humidified between the DMAs) were run on an approximately weekly basis in order to monitor the size offset between the two DMAs and to define the width of the DMA transfer functions (Gysel et al., 2009). The HTDMA was further verified by sampling nebulised ammonium sulphate, monitoring the growth factors for a range of RH (68% to 92%) at a given size (140

Atmos. Chem. Phys. Discuss., doi:10.5194/acp-2015-1020, 2016
Manuscript under review for journal Atmos. Chem. Phys.
Published: 18 January 2016

Atmospheric Chemistry and Physics Discussions

nm), and comparing to modelled values (ADDEM; Topping et al., 2005). More details of the calibration procedures for this instrument are given by Good et al. (2010).

2.3 CCNc measurements

The CCNc (Roberts and Nenes, 2005) operated downstream of a DMA (model 3081, TSI), the voltage of which was controlled with a classifier (TSI, model 3080) stepping discretely through a size range 16 nm to 325 nm. This quasi-monodisperse aerosol sample flow was then split isokinetically between the CCNc and a CPC (TSI, model 3010). The flow into the CPC was further diluted with filtered air by a factor of 2 in order to match the flow into the CCNc. Inside the CCNc, the aerosol flowed through a wetted column with a temperature gradient, providing supersaturated conditions in which a proportion of the particles activated and were detected by an Optical Particle Counter (OPC) at the bottom of the column. Throughout the deployment, the CCNc cycled through 5 calibrated supersaturation setpoints: 0.15%, 0.26%, 0.47%, 0.80% and 1.13%. The ratio of activated particles to total particles (measured by the CPC), can be determined as a function of dry particle diameter and supersaturation (the activated fraction: AF). By fitting a sigmoid curve function to this activation spectrum, the dry diameter at which 50% of particles activate (D_{50}) was derived. The hygroscopicity parameter, κ (Petters and Kreidenweis, 2007), was then derived from D_{50} and supersaturation using the κ-Köhler model. In addition, the total number of CCN (N_{CCN}) was calculated by integrating the number size distribution above D_{50}.

As with the HTDMA, the DMA was calibrated using nebulised latex spheres. The CCNc was calibrated by flowing nebulised ammonium sulphate into the system and determining the supersaturation at which 50% of the particles of a given dry size activate. This critical supersaturation is then compared to modelled values (ADDEM; Topping et al., 2005) to determine the slope and offset.

2.4 Bio-aerosol measurements

Fluorescent Biological Aerosol Particles (FBAP) in the size range $0.5 \leq D_p \leq 20\ \mu\mathrm{m}$ were detected using the WIBS-3M (Kaye et al., 2005; Foot et al., 2008; Stanley et al., 2011), which operates on the principle of ultraviolet light induced fluorescence of molecules common to most biological material, specifically Tryptophan and NADH. Two sequential pulses of UV light are provided by filtered Xenon lamps at 280 nm and 370 nm to excite Tryptophan and NADH, respectively. Fluorescence is then detected in the ranges 310–400 nm and 400–600 nm following the Tryptophan excitation, and 400–600 nm following the NADH excitation (i.e. 3 fluorescence channels).

The baseline fluorescence of the instrument is measured during so-called forced trigger (FT) sampling periods, where the instrument triggers the flash lamps and records the resultant fluorescence in the absence of aerosol in the sample volume. The mean fluorescence in a FT period is treated as the baseline fluorescence of the optical chamber during the sample period. For a particle to be considered fluorescent (FBAP) it must exhibit a fluorescence greater than a threshold value, defined as the baseline fluorescence plus 3 standard deviations, in any channel.

Size calibration of the WIBS-3M consisted of using latex spheres with a physical diameter of 1.0 µm. Blue fluorescent latex spheres (1.0 µm diameter) were also used to monitor the instrument fluorescent channel efficiencies and baseline with

Atmos. Chem. Phys. Discuss., doi:10.5194/acp-2015-1020, 2016
Manuscript under review for journal Atmos. Chem. Phys.
Published: 18 January 2016

Atmospheric Chemistry and Physics Discussions

time. The WIBS-3M inlet was operated at a total flow rate of 2.3 lpm (±5%). 90% of this was directed through a HEPA filter and used as a sheath flow, constraining the remaining 0.23 lpm for the scattering chamber sample flow from which particle concentrations were derived.

Particles detected by this instrument are termed FBAP, as they represent a lower limit of PBAP, some of which will not necessarily be detected by this method (Gabey et al., 2010; Huffman et al., 2012). This instrument has previously been deployed in Borneo, and further details of its operation are given by Gabey et al. (2010). In this experiment, the instrument was positioned in a small clearing, a few metres away from the rainforest understorey.

2.5 Removal of pollution episodes

While the site is described as pristine, it can nevertheless be affected by local emissions and regional transport of pollutants: biomass burning emissions from outside the reserve; the urban plume from Manaus; and pollution from the nearby diesel generator.

For each day of the campaign 7-day back trajectories were calculated using the HYSPLIT model (Draxler and Hess, 1998) at 30 minute intervals and 6 altitudes above TT34 (0, 250, 500, 1000, 2000 and 4000 m.a.s.l). The horizontal and vertical wind fields employed here were from the NCEP/NOAA 1°x 1°Global Data Assimilation System (GDAS) reanalysis product. These back trajectories were used to identify air masses arriving at TT34 which had either passed over Manaus or passed nearby active fire zones. A bounding box was drawn between -3.16°to -2.88°longitude and -60.12°to -59.81°longitude to define the Manaus influence zone, and any back trajectory passing over this box at any altitude was flagged.

Air masses potentially impacted by biomass burning were identified by coupling the back trajectory measurements to satellite detected fires as measured by the MODIS instrument. This operates on the Aqua and Terra satellites, which have local overpass times in the morning and afternoon respectively. The fire detection data (specific product: MCD14ML) was produced by the University of Maryland and acquired from the online Fire Information for Resource Management System (FIRMS; https://earthdata.nasa.gov/data/near-real-time-data/firms/about). At each location along the back trajectories the surrounding 1°box was interrogated for any fire counts at the nearest terra/aqua overpass. If any were present this trajectory was flagged as potentially influenced by biomass burning. This technique is subject to uncertainties associated with trajectory errors (e.g. Fleming et al., 2012) and the detection of fires in cloudy scenes, or false detection of fires (Schroeder et al., 2008), and therefore can only be considered qualitative.

Finally, data were flagged for possible contamination from the generator if the local wind direction was in the range 270°-340°.

In the event of any flag, the black carbon data (from the MAAP) were checked along with the particle counts (where available), and aerosol data were excluded if the pollution flag coincided with a significant increase in these concentrations. Approximately 28% of the HTDMA and CCNc data were removed in this way, with 5% of the data being flagged as possibly impacted by biomass burning and most of the rest due to the Manaus urban plume.

Atmos. Chem. Phys. Discuss., doi:10.5194/acp-2015-1020, 2016
Manuscript under review for journal Atmos. Chem. Phys.
Published: 18 January 2016

Atmospheric Chemistry and Physics Discussions

3 Results and Discussion

3.1 Size distributions

The particle number size distribution recorded over the measurement period of this study can be seen in fig. 1. This shows a broad accumulation mode peak at 130 - 150 nm with a median number concentration of 266 cm^{-3} (calculated from the integral of the size distribution curve). Despite observing aerosol number concentrations comparable to previous observations during the wet season, the shape of the distribution resembles those measured in the dry season Artaxo et al. (2013).

The size distribution, however, was quite variable over the period of the measurements, as can be seen in the time-series in fig. 2, and varied with total particle counts. Median size distributions observed when the total number concentration was above or below 200 cm^{-3} are shown in fig. 3. During periods of low particle counts, an Aitken mode is also seen, with a mode around 80 nm, while the size distribution during episodes of higher concentrations is dominated by the accumulation mode, possibly masking the smaller mode. Such a size distribution profile, dominated by accumulation mode aerosols, has also been reported during the dry season in western Amazonia, in the deforestation arc, during biomass burning events (Brito et al., 2014).

3.2 Composition

Submicron non-refractory aerosol composition, as measured by the ACSM during the period of this study, is illustrated in fig. 5. The mean mass loadings for organic material, sulphate and nitrate were 2.13 $\pm$ 0.75 µg m^{-3}, 0.11 $\pm$ 0.04 µg m^{-3}, 0.08 $\pm$ 0.03 µg m^{-3}, respectively ($\pm$ 1 standard deviation). Organic material dominated the submicron aerosol, comprising around 86% of the total mass, on average. Such a high fraction of organics compares well with previous observations in the Amazon basin (Artaxo et al., 2013; Brito et al., 2014; Andreae et al., 2015).

Levoglucosan, a major constituent of biomass burning aerosol, fragments in AMS and ACSM instruments at a mass-to-charge ratio (m/z) of 60 (Alfarra et al., 2007), and so the fraction f_{60} is frequently used as a marker for biomass burning (Artaxo et al., 2013; Chen et al., 2009). The mean f_{60} at TT34 in July 2013 was 0.19% $\pm$ 0.07%. This is well below 0.3%, which is considered to be the upper limit for background air masses not affected by biomass burning (Cubison et al., 2011), indicating that, on average, these measurements were not strongly impacted by local biomass burning emissions.

3.3 Aerosol water uptake

The HTDMA ran from the 13th to the 28th July. Figure 4 shows the time-series of RH-corrected GF distributions for all dry sizes, as derived from the HTDMA data using the TDMAinv toolkit. These largely exhibit a single mode at each size, which varied little over the period of measurements, roughly in the range 1.2 - 1.4. Smaller, more hygroscopic modes can be seen at the lower dry diameters, while the larger particles also show a hydrophobic mode in the growth factor distribution. The contribution of the hydrophobic mode to the larger particles is small ($<$ 10% in number) and may be due to a local anthropogenic influence that was not accounted for. The averages of the growth factor at the peak of this distribution (i.e. the dominant mode) are shown in table 1 and fig. 1. They show an increase with dry diameter, reflecting the difference between Aitken and accumulation mode

Atmos. Chem. Phys. Discuss., doi:10.5194/acp-2015-1020, 2016
Manuscript under review for journal Atmos. Chem. Phys.
Published: 18 January 2016

Atmospheric Chemistry and Physics Discussions

aerosol: organic mass fractions are highest in the Aitken mode, while elevated sulphate mass fractions have been previously seen in the accumulation mode (Gunthe et al., 2009; Pöschl et al., 2010). It should be noted, however, that the elevated sulphate events observed by Gunthe et al. (2009) were likely linked to long-range transport of biomass burning aerosol from Africa, which, due to a combination the African burning season and large scale circulation, tends to impact the Amazon forest more often during the wet season (Ben-Ami et al., 2010).

The campaign averages of the CCNc derived parameters, D_{50}, κ and N_{CCN} are given for each set supersaturation in table 2. The κ values are also plotted against D_{50} in fig. 1. Consistent with the growth factor data, and with previous measurements at this site (Gunthe et al., 2009), they show more hygroscopic particles at larger diameters $\kappa \approx 0.12$ below 100 nm, and $\kappa \approx 0.18$ around the accumulation mode.

Reconciliation between sub- and super-saturated particle water uptake for these measurements has already been investigated by Whitehead et al. (2014). They showed that there was agreement within the variability of the data, with a slightly underestimated hygroscopicity from the HTDMA data compared to the CCNc at lower supersaturations (larger dry diameters). The analysis of Whitehead et al. (2014) considered the full dataset without separating out the pollution events, however performing the same analysis on the 'clean' data did not result in any significant difference.

3.4 FBAP measurements

Measurements of biological particles in the Amazon are important as they are considered to have a strong influence on clouds as ice nuclei (Pöschl et al., 2010). The WIBS-3 operated uninterrupted from the morning of the 3rd July until 10th July. The mean total particle number concentration of FBAP measured by the WIBS-3 during this period was $475 \pm 244\ \mathrm{l}^{-1}$ (1 standard deviation), while the mean FBAP number concentration was $404 \pm 237\ \mathrm{l}^{-1}$ (i.e. accounting for 85% of the particles in the size range of the instrument). The time-series of number concentrations for the duration of this period is shown in fig. 6. This shows coarse mode particles were dominated by FBAP number concentrations, which exhibited a strong diurnal cycle with concentrations varying from around $200\ \mathrm{l}^{-1}$ during the daytime up to as much as $1200\ \mathrm{l}^{-1}$ at night. The diurnal variation (fig. 7) shows that FBAP number concentrations plateaued from around 21:00 through the night, began to drop from 05:00, reached a minimum by 11:00 and started increasing again from 15:00. The FBAP fraction was highest (more than 90%) at night, and remained high until around 08:00 - even after FBAP number concentrations began decreasing. This dropped to between 55% and 75% during the day, helped in part by an apparent increase in non-FBAP concentrations, before steadily increasing in line with the FBAP concentrations through the late afternoon / early evening.

There are a number of factors driving the diurnal cycle in coarse mode particles, as discussed by Huffman et al. (2012). Previous studies at this and a nearby site, utilizing electron and light microscopy, have identified the FBAP as predominantly fungal spores (Graham, 2003; Huffman et al., 2012). Similar diurnal cycles have been seen in airborne fungal spore densities at other tropical rainforest locations (Gilbert and Reynolds, 2005; Elbert et al., 2007). The observed night-time peak in FBAP number concentrations in fig. 7 is consistent with nocturnal sporulation driven by increasing RH (see bottom panel). The dependence of fungal spore release on meteorological conditions, however, varies greatly according to species, and any relationship is non-trivial (Jones and Harrison, 2004). FBAP number concentrations begin dropping several hours before any

Atmos. Chem. Phys. Discuss., doi:10.5194/acp-2015-1020, 2016
Manuscript under review for journal Atmos. Chem. Phys.
Published: 18 January 2016

Atmospheric Chemistry and Physics Discussions

decrease in RH, and the FBAP fraction also remains high (fig. 7). This suggests that the morning decrease in FBAP is not necessarily due to a cessation of emission processes, but may also be the result of a break-up of the nocturnal boundary layer around sunrise (Whitehead et al., 2010; Huffman et al., 2012). Graham (2003) and Huffman et al. (2012) suggest that the night-time increase in coarse mode particles is due, at least in part, to the shallow nocturnal boundary layer. The slight increase in non-FBAP concentrations during the day may be a result of enhanced particle exchange through the canopy, facilitated by sporadic turbulent events, as described by Whitehead et al. (2010), bringing non-FBAP that had originated elsewhere into the space below canopy.

Figure 8 shows the number size distributions reported by the WIBS-3 during the measurement period. Again, FBAP clearly dominates the particle number concentrations for $D_p > 1$ µm, however non-FBAP concentrations are higher for submicron particles. The FBAP number size distribution shows a peak at around 1.8 µm, while the non-FBAP distribution is characterized by a flatter, broader peak between 0.8 and 1.3 µm. Non-fluorescent particles at this site have previously been identified as mineral dust, non-fluorescent biological aerosol, and inorganic salts (Huffman et al., 2012).

A Ward linkage cluster analysis using the z-score normalisation was applied to the data, as described by Crawford et al. (2015), where the optimum number of retained distinct clusters was determined using the Calinski–Harabasz criterion. This analysis revealed three distinct fluorescent classes of particles (Cl1-3). Cl1 has previously been attributed to fungal spores (Crawford et al., 2014) based on comparison with other sampling techniques and the diurnal emission pattern (see fig. 7) with higher concentrations observed overnight. Cl2 appears to be a distinct sub-class of somewhat less fluorescent particles which remain unclassified, but shows similar behaviour to, and correlates strongly (r^2 = 0.86) with Cl1, hence both have been combined in fig. 7. Both clusters show similar fluorescent signatures to the clusters attributed to fungal spores by Crawford et al. (2014, 2015). The statistical parameters of each cluster are shown in table 3 for comparison. Together, these clusters contribute approximately 70% to the total fluorescent particle concentration, with no significant diurnal variation in this figure, suggesting that FBAP were dominated by fungal spores during this study. A third cluster, Cl3, shows very low concentrations (around 20 l^{-1}), with no strong diurnal trend, however there is insufficient data to speculate upon the nature of this cluster.

3.5 Comparison with previous studies

3.5.1 Submicron aerosol

Aerosol water-uptake studies have previously been conducted at the TT34 site by Gunthe et al. (2009) using size-selected CCNc measurements, and at Balbina (110 km NE of TT34) by Zhou et al. (2002) using a HTDMA, both during the wet season. HTDMA and CCNc measurements were also made at Balbina during the transition from wet to dry season by Rissler et al. (2004). In addition, HTDMA measurements from pasture-land in SW Amazonia at the end of the dry season / beginning of wet season are presented by Rissler et al. (2006) and Vestin et al. (2007). This study represents the first measurements with HTDMA and monodisperse CCN instruments at TT34 during the transition from wet to dry seasons. Concurrent CCNc and HTDMA measurements have also been conducted in Borneo, SE Asia, by Irwin et al. (2011), providing a useful comparison with a different tropical rainforest region.

Atmos. Chem. Phys. Discuss., doi:10.5194/acp-2015-1020, 2016
Manuscript under review for journal Atmos. Chem. Phys.
Published: 18 January 2016

Atmospheric Chemistry and Physics Discussions

The HTDMA growth factor measurements of Zhou et al. (2002) showed a similar pattern to this study: a dominant mode of "less hygroscopic" particles, accompanied at times by a hydrophobic mode (particularly at the larger particle sizes), and a more hygroscopic mode. The growth factors of the less hygroscopic particles are compared in fig. 9, along with the other studies. All the measurements showed a similar increase in growth factor with dry diameter. The growth factor values from this study were slightly higher than those of Zhou et al. (2002) and Rissler et al. (2004), but the difference is within the variability of the measurements, and probably within the variability that has been seen between different HTDMA instruments (Duplissy et al., 2009; Massling et al., 2011). The "moderately hygroscopic" particles observed by Rissler et al. (2006) exhibited growth factors in the same range as the other studies in Amazonia, however in this case, the hydrophobic mode (GF $\approx$ 1.05 - 1.13) was dominant for all but the larger particles ($>$ 135 nm). Furthermore, strong diurnal cycles were observed (Rissler et al., 2006; Vestin et al., 2007), which were not seen during the current study. In contrast to the current study, the measurements of Rissler et al. (2006) and Vestin et al. (2007) were conducted in a region that has undergone heavy land use change and is strongly influenced by anthropogenic sources (Andreae et al., 2002), which may contribute to the observed diurnal pattern.

In contrast to the studies from Amazonia, aerosol growth factors measured in Borneo (Irwin et al., 2011) were somewhat higher: in the range 1.3 - 1.7 (fig. 9). This can be explained by the fact that, while the site in Amazon benefited from a fetch of hundreds of kilometres of undisturbed rainforest, the site in Borneo was heavily influenced by marine air masses (Robinson et al., 2011). As discussed by Robinson et al. (2011), the sulphate loadings in Borneo were substantially higher than in Amazonia, even in air masses from across the island, which, with sulphate being more hygroscopic than organic aerosol, would explain the higher growth factors.

The results of the humidogram are shown in fig. 10, and compared to the humidogram data from Borneo (Irwin et al., 2011) and the humidogram fit for the wet season data of Rissler et al. (2006). Growth factors in Borneo were higher across the RH range than in Amazonia. As with previous measurements, no deliquesence behaviour was seen in this study.

Values of κ derived from the HTDMA and CCNc measurements during these studies are compared in fig. 11, as a function of dry diameter. Here, the κ from HTDMA measurements is derived using the average growth factor, rather than the peak of the less hygroscopic mode, for direct comparison with the CCNc derived values. The various measurements in Amazonia showed very similar κ, largely agreeing within the variability of the individual measurements. It can be said that water uptake measurements in Amazonia are consistent, and, as noted by Gunthe et al. (2009), show κ to be around half that typically seen in other continental regions (Andreae and Rosenfeld, 2008).

The HTDMA derived κ from the Borneo experiment shows more hygroscopic aerosol than in Amazonia, as discussed above, however the CCNc derived values are more in line with those in Amazonia. This discrepancy has been noted previously and possible reasons for it discussed by Irwin et al. (2011) and Whitehead et al. (2014).

In general, the particle concentrations and hygroscopic properties observed during this study were similar to those seen during wet season measurements in the Amazon rainforest. Under these conditions, cloud droplet formation in convective clouds in this region is likely to be aerosol- limited (Reutter et al., 2009). Previous modelling studies have suggested this is the case during the wet season (Pöschl et al., 2010), in contrast to the dry season during periods of intense biomass burning when droplet number is largely controlled by the updraft velocity (Reutter et al., 2009).

Atmos. Chem. Phys. Discuss., doi:10.5194/acp-2015-1020, 2016
Manuscript under review for journal Atmos. Chem. Phys.
Published: 18 January 2016

Atmospheric Chemistry and Physics Discussions

3.5.2 Coarse mode aerosol

Huffman et al. (2012) conducted measurements of FBAP at the TT34 tower using an ultraviolet aerodynamic particle sizer (UV-APS) during the AMAZE-08 campaign. In contrast to this study, the AMAZE-08 measurements were taken during the wet season (February to March), from the top of the tower (i.e. above canopy). It is also worth comparing with the measurements of Gabey et al. (2010), who used the same WIBS-3 instrument to sample the aerosol above and below canopy in the rainforest of north-east Borneo.

The median number concentration of FPAB observed below the canopy in this study was 372 l^{-1}, while the UV-APS measurements at the top of the tower by Huffman et al. (2012) were around a fifth of this, at 73 l^{-1} (also median). In an intercomparison between the two different measurement techniques, Healy et al. (2014) found that, while there was agreement in total number concentrations, the counts in the fluorescence channels of the WIBS (particularly FL1) were substantially higher than the UV-APS fluoresence counts, which would at least partly explain the difference here. Meteorological conditions would be expected to favour emission during the wet season measurement period of Huffman et al. (2012). At other locations, Gabey et al. (2010) saw concentrations often in excess of 1500 l^{-1} below canopy, and around 200 l^{-1} above, using the same instrument at each site, while Gilbert and Reynolds (2005) observed substantially higher concentrations of fungal spores in the understorey than in the canopy during measurements in Queensland, Australia. Strong vertical gradients in biological particles are therefore regularly seen in rainforest environments, and would be an additional factor in the differences observed between the measurements at TT34.

The fraction of FBAP in this study was, on average 85% of total coarse mode particles (and as much as 90%) whereas it was 24% in the AMAZE-08 campaign (41% in unpolluted conditions). The higher fraction at ground level would be expected, being closer to the source, whereas above canopy, there is a stronger influence from non-fluorescent particles from external sources. In Borneo, as in the Amazon, there was a higher fraction below the canopy (55%) than above (28%), however not as high as the 85% observed in this study. Reasons for this difference are unclear, but may include a stronger influence in Borneo of non-fluorescent particles from external sources, such as the nearby coast.

One difference between the measurements of this study and others is the position of the mode in the FBAP number size distribution. Gabey et al. (2010) report the peak at 2.5 µm, while Huffman et al. (2012) observe the peak around 2.3 µm. By contrast, the peak in this study was 1.8 µm. The difference between the two measurements at TT34 is likely due to the different measurement techniques, with the UV-APS found to be less sensitive to smaller fluorescent particles (Healy et al., 2014).

Diurnal variations between this study and that of Huffman et al. (2012) were similar, however Gabey et al. (2010) reported an additional increase in the afternoon in Borneo. This increase coincided with a peak in RH, and it is believed that this is linked (Gabey et al., 2010). In this study, the RH increased more gradually through the afternoon and evening (see fig. 7, bottom panel), which may explain the lack of afternoon peak in FBAP compared to the Borneo results. Huffman et al. (2012) also don't observe a mid-afternoon peak in FBAP.

Atmos. Chem. Phys. Discuss., doi:10.5194/acp-2015-1020, 2016
Manuscript under review for journal Atmos. Chem. Phys.
Published: 18 January 2016

Atmospheric Chemistry and Physics Discussions

4 Conclusions

Measurements of aerosol concentrations and water uptake properties were conducted at a remote site in pristine Amazonian rainforest in July, 2013, during the transition from the wet to dry seasons. Back trajectories and wind sectors were examined in conjunction with black carbon concentrations in order to exclude any pollution episodes and ensure the aerosol measured were representative of background aerosol over the rainforest.

In the absence of polluted periods, particle concentrations were low, with a median of 266 cm^{-3}. The particle size distributions were largely dominated by an accumulation mode around 130 - 150 nm, with a smaller Aitken mode apparent during periods of lower particle counts. Based on previous measurements contrasting wet and dry seasons (Artaxo et al., 2013), the results here may reflect the transition between the two seasons, with periods consistent with each at different times (but without any influence from biomass burning).

Aerosol water uptake and hygroscopicity was measured using an HTDMA and a CCNc. Good agreement was found between the measurements of both instruments. Particle growth factors from the HTDMA varied little over most of the measurement period and were typically between 1.2 and 1.4 (low hygroscopicity mode). Aerosol hygroscopicity was found to be low (κ = 0.12) for Aitken mode particles, and increased slightly to κ = 0.18 for accumulation mode particles. This is consistent with previous measurements at, or near this site, and with the observation that Aitken mode particle composition is dominated by organic material, while accumulation mode particles exhibited higher sulphate mass fractions (Pöschl et al., 2010).

Particles in the size range $0.5 \leq D_p \leq 20$ µm were measured using the WIBS-3M, which distinguishes fluorescent (representing a subset of primary biological aerosols, or FBAP) and non-fluorescent. FBAP dominated the coarse mode aerosol, accounting for as much as 90%. Concentrations of FBAP followed a strong diurnal cycle, with maximum concentrations during the night. This is likely driven by a combination of the dependence of emission processes on meteorological conditions and the diurnal cycle of the boundary layer.

The results from this study were also compared to measurements conducted in Borneo in 2008 (Irwin et al., 2011; Gabey et al., 2010; Robinson et al., 2011), contrasting the vast 'Green Ocean' of the Amazon rainforest to the island rainforest geography of SE Asia. In the submicron range, aerosol hygroscopicity was greater in Borneo, possibly due to the stronger marine influence of that region (Irwin et al., 2011). Coarse mode particles at both locations were dominated by FBAP (probably mostly fungal spores). Below canopy, the Amazon exhibited a higher fraction of FBAP than Borneo, though higher FBAP concentrations were seen at the latter.

Acknowledgements. The authors wish to thank the Large-scale Biosphere-Atmosphere (LBA) project group at the National Institute for Amazonian Research (INPA) in Manaus, for logistical support before and during the field deployment. The Brazil-UK Network for Investigation of Amazonian Atmospheric Composition and Impacts on Climate project was funded by the UK Natural Environment Research Council (NERC; grant: NE/I030178/1). NERC also funded the Ph.D. studentship of E. Darbyshire. J. Brito was funded by Fundação de Amparo à Pesquisa do Estado de São Paulo (FAPESP; project 2013/25058-1).

Atmos. Chem. Phys. Discuss., doi:10.5194/acp-2015-1020, 2016
Manuscript under review for journal Atmos. Chem. Phys.
Published: 18 January 2016

References

Alfarra, M. R., Prevot, A. S. H., Szidat, S., Sandradewi, J., Weimer, S., Lanz, V. A., Schreiber, D., Mohr, M., and Baltensperger, U.: Identification of the Mass Spectral Signature of Organic Aerosols from Wood Burning Emissions, Environmental Science & Technology, 41, 5770–5777, doi:10.1021/es062289b, 2007.

Allan, J. D., Morgan, W. T., Darbyshire, E., Flynn, M. J., Williams, P. I., Oram, D. E., Artaxo, P., Brito, J., Lee, J. D., and Coe, H.: Airborne observations of IEPOX-derived isoprene SOA in the Amazon during SAMBBA, Atmospheric Chemistry and Physics, 14, 11 393–11 407, doi:10.5194/acp-14-11393-2014, http://www.atmos-chem-phys.net/14/11393/2014/, 2014.

Andreae, M. and Rosenfeld, D.: Aerosol–cloud–precipitation interactions. Part 1. The nature and sources of cloud-active aerosols, Earth-Science Reviews, 89, 13–41, doi:10.1016/j.earscirev.2008.03.001, 2008.

Andreae, M. O., Artaxo, P., Brandão, C., Carswell, F. E., Ciccioli, P., Da Costa, A. L., Gulf, A. D., Esteves, J. L., Gash, J. H. C., Grace, J., Kabat, P., Lelieveld, J., Malhi, Y., Manzi, A. O., Meixner, F. X., Nobre, A. D., Nobre, C., Ruivo, M. D. L. P., Silva-Dias, M. A., Stefani, P., Valentini, R., Von Jouanne, J., and Waterloo, M. J.: Biogeochemical cycling of carbon, water, energy, trace gases, and aerosols in Amazonia: The LBA-EUSTACH experiments, Journal of Geophysical Research D: Atmospheres, 107, 8066, doi:10.1029/2001JD000524, 2002.

Andreae, M. O., Rosenfeld, D., Artaxo, P., Costa, A. A., Frank, G. P., Longo, K. M., and Silva-Dias, M. A. F.: Smoking rain clouds over the Amazon., Science (New York, N.Y.), 303, 1337–42, doi:10.1126/science.1092779, 2004.

Andreae, M. O., Acevedo, O. C., Araùjo, A., Artaxo, P., Barbosa, C. G. G., Barbosa, H. M. J., Brito, J., Carbone, S., Chi, X., Cintra, B. B. L., da Silva, N. F., Dias, N. L., Dias-Júnior, C. Q., Ditas, F., Ditz, R., Godoi, A. F. L., Godoi, R. H. M., Heimann, M., Hoffmann, T., Kesselmeier, J., Könemann, T., Krüger, M. L., Lavric, J. V., Manzi, A. O., Moran-Zuloaga, D., Nölscher, A. C., Santos Nogueira, D., Piedade, M. T. F., Pöhlker, C., Pöschl, U., Rizzo, L. V., Ro, C.-U., Ruckteschler, N., Sá, L. D. A., Sá, M. D. O., Sales, C. B., Santos, R. M. N. D., Saturno, J., Schöngart, J., Sörgel, M., de Souza, C. M., de Souza, R. A. F., Su, H., Targhetta, N., Tóta, J., Trebs, I., Trumbore, S., van Eijck, A., Walter, D., Wang, Z., Weber, B., Williams, J., Winderlich, J., Wittmann, F., Wolff, S., and Yáñez Serrano, A. M.: The Amazon Tall Tower Observatory (ATTO) in the remote Amazon Basin: overview of first results from ecosystem ecology, meteorology, trace gas, and aerosol measurements, Atmospheric Chemistry and Physics Discussions, 15, 11 599–11 726, doi:10.5194/acpd-15-11599-2015, 2015.

Artaxo, P., Rizzo, L. V., Brito, J. F., Barbosa, H. M. J., Arana, A., Sena, E. T., Cirino, G. G., Bastos, W., Martin, S. T., and Andreae, M. O.: Atmospheric aerosols in Amazonia and land use change: from natural biogenic to biomass burning conditions, Faraday Discussions, 165, 203, doi:10.1039/c3fd00052d, 2013.

Ben-Ami, Y., Koren, I., Rudich, Y., Artaxo, P., Martin, S. T., and Andreae, M. O.: Transport of North African dust from the Bodélé depression to the Amazon Basin: a case study, Atmospheric Chemistry and Physics, 10, 7533–7544, doi:10.5194/acp-10-7533-2010, 2010.

Brito, J., Rizzo, L. V., Morgan, W. T., Coe, H., Johnson, B., Haywood, J., Longo, K., Freitas, S., Andreae, M. O., and Artaxo, P.: Ground-based aerosol characterization during the South American Biomass Burning Analysis (SAMBBA) field experiment, Atmospheric Chemistry and Physics, 14, 12 069–12 083, doi:10.5194/acp-14-12069-2014, 2014.

Chen, Q., Farmer, D. K., Schneider, J., Zorn, S. R., Heald, C. L., Karl, T. G., Guenther, A., Allan, J. D., Robinson, N., Coe, H., Kimmel, J. R., Pauliquevis, T., Borrmann, S., Pöschl, U., Andreae, M. O., Artaxo, P., Jimenez, J. L., and Martin, S. T.: Mass spectral characterization of submicron biogenic organic particles in the Amazon Basin, Geophysical Research Letters, 36, L20 806, doi:10.1029/2009GL039880, 2009.

Chen, Q., Farmer, D. K., Rizzo, L. V., Pauliquevis, T., Kuwata, M., Karl, T. G., Guenther, A., Allan, J. D., Coe, H., Andreae, M. O., Pöschl, U., Jimenez, J. L., Artaxo, P., and Martin, S. T.: Submicron particle mass concentrations and sources in the Amazonian wet season (AMAZE-08), Atmospheric Chemistry and Physics, 15, 3687–3701, doi:10.5194/acp-15-3687-2015, 2015.

Crawford, I., Robinson, N. H., Flynn, M. J., Foot, V. E., Gallagher, M. W., Huffman, J. A., Stanley, W. R., and Kaye, P. H.: Characterisation of bioaerosol emissions from a Colorado pine forest: results from the BEACHON-RoMBAS experiment, Atmospheric Chemistry and Physics, 14, 8559–8578, doi:10.5194/acp-14-8559-2014, 2014.

Crawford, I., Ruske, S., Topping, D. O., and Gallagher, M. W.: Evaluation of hierarchical agglomerative cluster analysis methods for discrimination of primary biological aerosol, Atmospheric Measurement Techniques, 8, 4979–4991, doi:10.5194/amt-8-4979-2015, 2015.

Cubison, M., Coe, H., and Gysel, M.: A modified hygroscopic tandem DMA and a data retrieval method based on optimal estimation, Journal of Aerosol Science, 36, 846–865, doi:10.1016/j.jaerosci.2004.11.009, 2005.

Cubison, M. J., Ortega, A. M., Hayes, P. L., Farmer, D. K., Day, D., Lechner, M. J., Brune, W. H., Apel, E., Diskin, G. S., Fisher, J. A., Fuelberg, H. E., Hecobian, A., Knapp, D. J., Mikoviny, T., Riemer, D., Sachse, G. W., Sessions, W., Weber, R. J., Weinheimer, A. J., Wisthaler, A., and Jimenez, J. L.: Effects of aging on organic aerosol from open biomass burning smoke in aircraft and laboratory studies, Atmospheric Chemistry and Physics, 11, 12 049–12 064, doi:10.5194/acp-11-12049-2011, 2011.

Draxler, R. and Hess, G.: An Overview of the HYSPLIT_4 Modelling System for Trajectories, Dispersion, and Deposition, Australian Meteorological Magazine, 47, 295–308, 1998.

Duplissy, J., Gysel, M., Sjogren, S., Meyer, N., Good, N., Kammermann, L., Michaud, V., Weigel, R., Martins dos Santos, S., Gruening, C., Villani, P., Laj, P., Sellegri, K., Metzger, A., McFiggans, G. B., Wehrle, G., Richter, R., Dommen, J., Ristovski, Z., Baltensperger, U., and Weingartner, E.: Intercomparison study of six HTDMAs: results and recommendations, Atmospheric Measurement Techniques, 2, 363–378, doi:10.5194/amt-2-363-2009, 2009.

Elbert, W., Taylor, P. E., Andreae, M. O., and Pöschl, U.: Contribution of fungi to primary biogenic aerosols in the atmosphere: wet and dry discharged spores, carbohydrates, and inorganic ions, Atmospheric Chemistry and Physics, 7, 4569–4588, doi:10.5194/acp-7-4569-2007, 2007.

Fleming, Z. L., Monks, P. S., and Manning, A. J.: Review: Untangling the influence of air-mass history in interpreting observed atmospheric composition, Atmospheric Research, 104-105, 1–39, doi:10.1016/j.atmosres.2011.09.009, 2012.

Foot, V. E., Kaye, P. H., Stanley, W. R., Barrington, S. J., Gallagher, M., and Gabey, A.: Low-cost real-time multiparameter bioaerosol sensors, in: Proceedings of SPIE, edited by Carrano, J. C. and Zukauskas, A., vol. 7116, pp. 71 160I–71 160I–12, SPIE, doi:10.1117/12.800226, 2008.

Formenti, P., Andreae, M. O., Lange, L., Roberts, G., Cafmeyer, J., Rajta, I., Maenhaut, W., Holben, B. N., Artaxo, P., and Lelieveld, J.: Saharan dust in Brazil and Suriname during the Large-Scale Biosphere-Atmosphere Experiment in Amazonia (LBA) - Cooperative LBA Regional Experiment (CLAIRE) in March 1998, Journal of Geophysical Research, 106, 14 919, doi:10.1029/2000JD900827, 2001.

Gabey, A. M., Gallagher, M. W., Whitehead, J., Dorsey, J. R., Kaye, P. H., and Stanley, W. R.: Measurements and comparison of primary biological aerosol above and below a tropical forest canopy using a dual channel fluorescence spectrometer, Atmospheric Chemistry and Physics, 10, 4453–4466, doi:10.5194/acp-10-4453-2010, 2010.

Gilbert, G. S. and Reynolds, D. R.: Nocturnal fungi: Airborne spores in the canopy and understory of a tropical rain forest, Biotropica, 37, 462–464, doi:10.1111/j.1744-7429.2005.00061.x, 2005.

Good, N., Coe, H., and McFiggans, G.: Instrumentational operation and analytical methodology for the reconciliation of aerosol water uptake under sub- and supersaturated conditions, Atmospheric Measurement Techniques, 3, 1241–1254, doi:10.5194/amt-3-1241-2010, 2010.

Graham, B.: Composition and diurnal variability of the natural Amazonian aerosol, Journal of Geophysical Research, 108, doi:10.1029/2003JD004049, 2003.

Gunthe, S. S., King, S. M., Rose, D., Chen, Q., Roldin, P., Farmer, D. K., Jimenez, J. L., Artaxo, P., Andreae, M. O., Martin, S. T., and Poschl, U.: Cloud condensation nuclei in pristine tropical rainforest air of Amazonia : size-resolved measurements and modeling of atmospheric aerosol composition and CCN activity, Atmospheric Chemistry and Physics, 9, 7551–7575, 2009.

Gysel, M., McFiggans, G., and Coe, H.: Inversion of tandem differential mobility analyser (TDMA) measurements, Journal of Aerosol Science, 40, 134–151, doi:10.1016/j.jaerosci.2008.07.013, 2009.

Healy, D. A., Huffman, J. A., O'Connor, D. J., Pöhlker, C., Pöschl, U., and Sodeau, J. R.: Ambient measurements of biological aerosol particles near Killarney, Ireland: a comparison between real-time fluorescence and microscopy techniques, Atmospheric Chemistry and Physics, 14, 8055–8069, doi:10.5194/acp-14-8055-2014, 2014.

Huffman, J. A., Sinha, B., Garland, R. M., Snee-Pollmann, A., Gunthe, S. S., Artaxo, P., Martin, S. T., Andreae, M. O., and Pöschl, U.: Size distributions and temporal variations of biological aerosol particles in the Amazon rainforest characterized by microscopy and real-time UV-APS fluorescence techniques during AMAZE-08, Atmospheric Chemistry and Physics, 12, 11 997–12 019, doi:10.5194/acp-12-11997-2012, 2012.

Irwin, M., Robinson, N., Allan, J. D., Coe, H., and McFiggans, G.: Size-resolved aerosol water uptake and cloud condensation nuclei measurements as measured above a Southeast Asian rainforest during OP3, Atmospheric Chemistry and Physics, 11, 11 157–11 174, doi:10.5194/acp-11-11157-2011, 2011.

Jones, A. M. and Harrison, R. M.: The effects of meteorological factors on atmospheric bioaerosol concentrations–a review., The Science of the total environment, 326, 151–80, doi:10.1016/j.scitotenv.2003.11.021, 2004.

Kaye, P. H., Stanley, W. R., Hirst, E., Foot, E. V., Baxter, K. L., and Barrington, S. J.: Single particle multichannel bio-aerosol fluorescence sensor, Optics Express, 13, 3583–3593, 2005.

Krejci, R., Ström, J., de Reus, M., Williams, J., Fischer, H., Andreae, M. O., and Hansson, H.-C.: Spatial and temporal distribution of atmospheric aerosols in the lowermost troposphere over the Amazonian tropical rainforest, Atmospheric Chemistry and Physics, 5, 1527–1543, doi:10.5194/acp-5-1527-2005, 2005.

Martin, S. T., Andreae, M. O., Althausen, D., Artaxo, P., Baars, H., Borrmann, S., Chen, Q., Farmer, D. K., Guenther, A., Gunthe, S. S., Jimenez, J. L., Karl, T., Longo, K., Manzi, A., Müller, T., Pauliquevis, T., Petters, M. D., Prenni, a. J., Pöschl, U., Rizzo, L. V., Schneider, J., Smith, J. N., Swietlicki, E., Tota, J., Wang, J., Wiedensohler, A., and Zorn, S. R.: An overview of the Amazonian Aerosol Characterization Experiment 2008 (AMAZE-08), Atmospheric Chemistry and Physics, 10, 11 415–11 438, doi:10.5194/acp-10-11415-2010, 2010a.

Martin, S. T., Andreae, M. O., Artaxo, P., Baumgardner, D., Chen, Q., Goldstein, A. H., Guenther, A., Heald, C. L., Mayol-Bracero, O. L., McMurry, P. H., Pauliquevis, T., Pöschl, U., Prather, K. A., Roberts, G. C., Saleska, S. R., Silva Dias, M. A., Spracklen, D. V., Swietlicki, E., and Trebs, I.: Sources and properties of Amazonian aerosol particles, Reviews of Geophysics, 48, RG2002, doi:10.1029/2008RG000280, 2010b.

Massling, A., Niedermeier, N., Hennig, T., Fors, E. O., Swietlicki, E., Ehn, M., Hämeri, K., Villani, P., Laj, P., Good, N., McFiggans, G., and Wiedensohler, A.: Results and recommendations from an intercomparison of six Hygroscopicity-TDMA systems, Atmospheric Measurement Techniques, 4, 485–497, doi:10.5194/amt-4-485-2011, 2011.

Petters, M. D. and Kreidenweis, S. M.: A single parameter representation of hygroscopic growth and cloud condensation nucleus activity, Atmospheric Chemistry and Physics, 7, 1961–1971, doi:10.1080/02786820701557214, 2007.

Pöschl, U., Martin, S. T., Sinha, B., Chen, Q., Gunthe, S. S., Huffman, J. A., Borrmann, S., Farmer, D. K., Garland, R. M., Helas, G., Jimenez, J. L., King, S. M., Manzi, A., Mikhailov, E., Pauliquevis, T., Petters, M. D., Prenni, A. J., Roldin, P., Rose, D., Schneider, J., Su, H., Zorn, S. R., Artaxo, P., and Andreae, M. O.: Rainforest aerosols as biogenic nuclei of clouds and precipitation in the Amazon., Science (New York, N.Y.), 329, 1513–6, doi:10.1126/science.1191056, 2010.

Prenni, A. J., Petters, M. D., Kreidenweis, S. M., Heald, C. L., Martin, S. T., Artaxo, P., Garland, R. M., Wollny, A. G., and Pöschl, U.: Relative roles of biogenic emissions and Saharan dust as ice nuclei in the Amazon basin, Nature Geoscience, 2, 402–405, 2009.

Reutter, P., Trentmann, J., Su, H., Simmel, M., Rose, D., Wernli, H., Andreae, M. O., and Pöschl, U.: Aerosol- and updraft-limited regimes of cloud droplet formation: influence of particle number, size and hygroscopicity on the activation of cloud condensation nuclei (CCN), Atmospheric Chemistry and Physics Discussions, 9, 8635–8665, doi:10.5194/acpd-9-8635-2009, 2009.

Rissler, J., Swietlicki, E., Zhou, J., Roberts, G., Andreae, M. O., Gatti, L. V., and Artaxo, P.: Physical properties of the sub-micrometer aerosol over the Amazon rain forest during the wet-to-dry season transition - comparison of modeled and measured CCN concentrations, Atmospheric Chemistry and Physics, 4, 2119–2143, doi:10.5194/acp-4-2119-2004, 2004.

Rissler, J., Vestin, A., Swietlicki, E., Fisch, G., Zhou, J., Artaxo, P., and Andreae, M. O.: Size distribution and hygroscopic properties of aerosol particles from dry-season biomass burning in Amazonia, Atmospheric Chemistry and Physics, 6, 471–491, 2006.

Rizzo, L. V., Artaxo, P., Müller, T., Wiedensohler, a., Paixão, M., Cirino, G. G., Arana, a., Swietlicki, E., Roldin, P., Fors, E. O., Wiedemann, K. T., Leal, L. S. M., and Kulmala, M.: Long term measurements of aerosol optical properties at a primary forest site in Amazonia, Atmospheric Chemistry and Physics, 13, 2391–2413, doi:10.5194/acp-13-2391-2013, 2013.

Roberts, G. C. and Nenes, A.: A Continuous-Flow Streamwise Thermal-Gradient CCN Chamber for Atmospheric Measurements, Aerosol Science and Technology, 39, 206–221, doi:10.1080/027868290913988, 2005.

Robinson, N. H., Newton, H. M., Allan, J. D., Irwin, M., Hamilton, J. F., Flynn, M., Bower, K. N., Williams, P. I., Mills, G., Reeves, C. E., McFiggans, G., and Coe, H.: Source attribution of Bornean air masses by back trajectory analysis during the OP3 project, Atmospheric Chemistry and Physics, 11, 9605–9630, doi:10.5194/acp-11-9605-2011, 2011.

Schroeder, W., Prins, E., Giglio, L., Csiszar, I., Schmidt, C., Morisette, J., and Morton, D.: Validation of GOES and MODIS active fire detection products using ASTER and ETM+ data, Remote Sensing of Environment, 112, 2711–2726, doi:10.1016/j.rse.2008.01.005, 2008.

Stanley, W. R., Kaye, P. H., Foot, V. E., Barrington, S. J., Gallagher, M., and Gabey, A.: Continuous bioaerosol monitoring in a tropical environment using a UV fluorescence particle spectrometer, Atmospheric Science Letters, 12, 195–199, doi:10.1002/asl.310, 2011.

Topping, D. O., McFiggans, G. B., and Coe, H.: A curved multi-component aerosol hygroscopicity model framework: Part 1 - Inorganic compounds, Atmospheric Chemistry and Physics, 5, 1205–1222, 2005.

Tuch, T. M., Haudek, A., Müller, T., Nowak, A., Wex, H., and Wiedensohler, A.: Design and performance of an automatic regenerating adsorption aerosol dryer for continuous operation at monitoring sites, Atmospheric Measurement Techniques, 2, 417–422, doi:10.5194/amt-2-417-2009, 2009.

Vestin, A., Rissler, J., Swietlicki, E., Frank, G. P., and Andreae, M. O.: Cloud-nucleating properties of the Amazonian biomass burning aerosol: Cloud condensation nuclei measurements and modeling, Journal of Geophysical Research, 112, D14 201, doi:10.1029/2006JD008104, 2007.

Whitehead, J. D., Gallagher, M. W., Dorsey, J. R., Robinson, N., Gabey, A. M., Coe, H., McFiggans, G., Flynn, M. J., Ryder, J., Nemitz, E., and Davies, F.: Aerosol fluxes and dynamics within and above a tropical rainforest in South-East Asia, Atmospheric Chemistry and Physics, 10, 9369–9382, 2010.

Atmos. Chem. Phys. Discuss., doi:10.5194/acp-2015-1020, 2016
Manuscript under review for journal Atmos. Chem. Phys.
Published: 18 January 2016

Atmospheric Chemistry and Physics Discussions

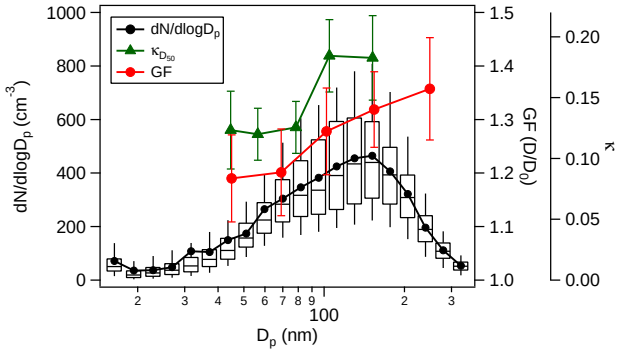

Figure 1. Particle number size distribution for the experiment. Box-and-whisker plots showing the median, interquartile ranges and 5th and 95th percentiles, and lines and markers showing mean $dN/dlogD_P$.

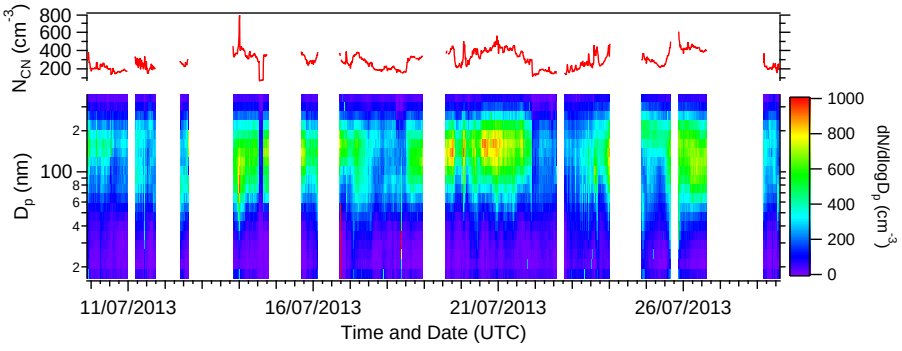

Figure 2. The time-series of particle number size distribution and total counts.

Whitehead, J. D., Irwin, M., Allan, J. D., Good, N., and McFiggans, G.: A meta-analysis of particle water uptake reconciliation studies, Atmospheric Chemistry and Physics, 14, 11 833–11 841, doi:10.5194/acp-14-11833-2014, 2014.

Worobiec, A., Szalóki, I., Osán, J., Maenhaut, W., Anna Stefaniak, E., and Van Grieken, R.: Characterisation of Amazon Basin aerosols at the individual particle level by X-ray microanalytical techniques, Atmospheric Environment, 41, 9217–9230, doi:10.1016/j.atmosenv.2007.07.056, 2007.

Zhou, J., Swietlicki, E., Hansson, H. C., and Artaxo, P.: Submicrometer aerosol particle size distribution and hygroscopic growth measured in the Amazon rain forest during the wet season, Journal of Geophysical Research, 107, 8055, doi:10.1029/2000JD000203, 2002.

Atmos. Chem. Phys. Discuss., doi:10.5194/acp-2015-1020, 2016
Manuscript under review for journal Atmos. Chem. Phys.
Published: 18 January 2016

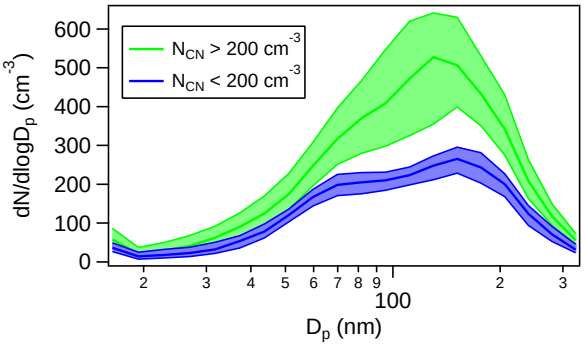

Figure 3. Median and interquartile ranges of particle number size distributions observed during high (> 200 cm^{-3}) and low (< 200 cm^{-3}) total particle number concentrations.

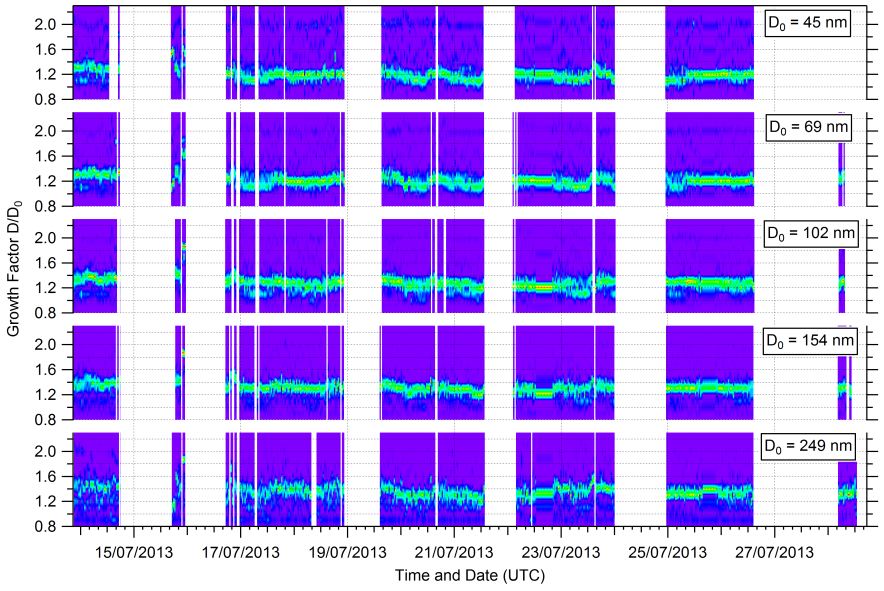

Figure 4. The time-series of normalised RH-corrected (to 90%) growth factor distributions derived from HTDMA measurements, for all 5 dry diameters. Gaps are largely due to removal of data from pollution episodes and humidograms.

Atmos. Chem. Phys. Discuss., doi:10.5194/acp-2015-1020, 2016
Manuscript under review for journal Atmos. Chem. Phys.
Published: 18 January 2016

Atmospheric Chemistry and Physics Discussions

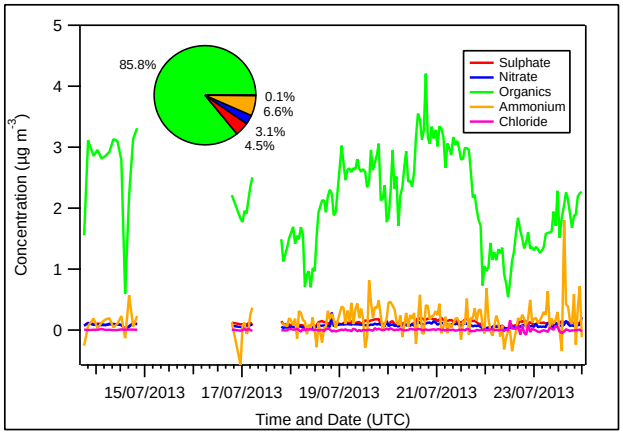

Figure 5. Submicron non-refractory aerosol composition from the ACSM measurements.

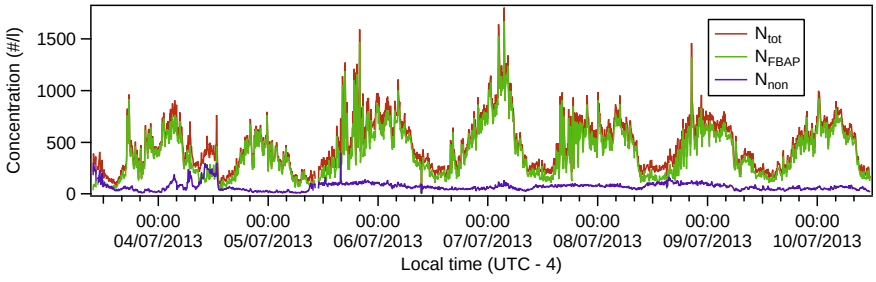

Figure 6. The time-series of total, FBAP and non-FBAP number concentrations.

Table 1. Mean peak growth factors and derived κ from HTDMA measurements for each dry diameter, along with $\pm$ standard deviation.

D0 (nm)	GF	κ
45	1.19 ± 0.08	0.09 ± 0.10
69	1.20 ± 0.08	0.09 ± 0.09
102	1.28 ± 0.08	0.12 ± 0.10
154	1.32 ± 0.07	0.15 ± 0.09
249	1.36 ± 0.10	0.17 ± 0.09

Atmos. Chem. Phys. Discuss., doi:10.5194/acp-2015-1020, 2016
Manuscript under review for journal Atmos. Chem. Phys.
Published: 18 January 2016

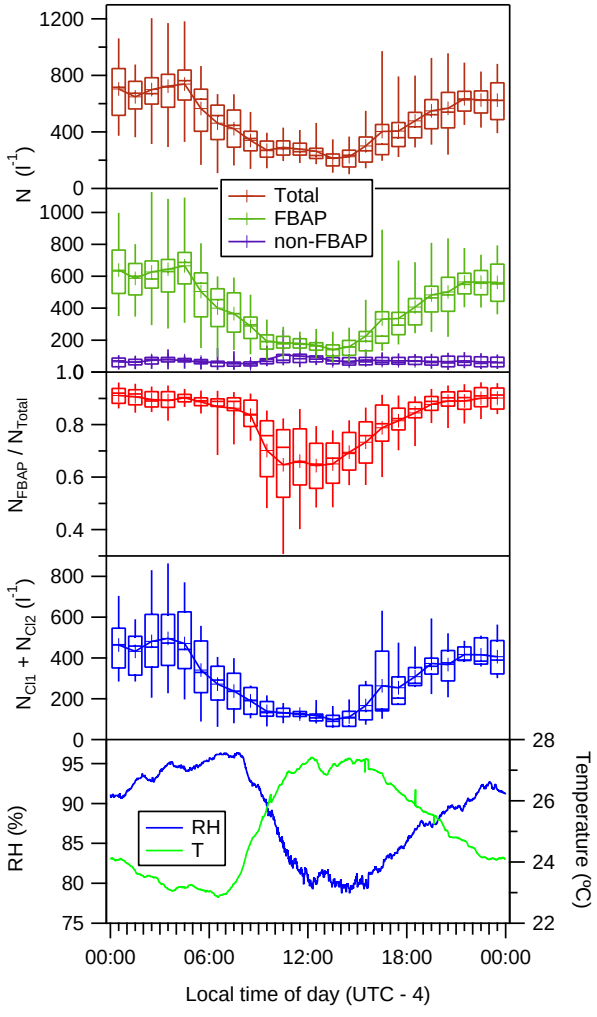

Figure 7. Diurnal variations in total, FBAP and non-FBAP number concentrations, as well as the fraction of FBAP, and the combined number concentrations of clusters Cl1 and Cl2. Shown are the means (lines and markers), medians and inter-quartile ranges (boxes) and 5th and 95th percentiles (whiskers). Also shown at the bottom are the mean diurnal variations in temperature and RH for the same period.

Atmos. Chem. Phys. Discuss., doi:10.5194/acp-2015-1020, 2016
Manuscript under review for journal Atmos. Chem. Phys.
Published: 18 January 2016

Atmospheric Chemistry and Physics Discussions

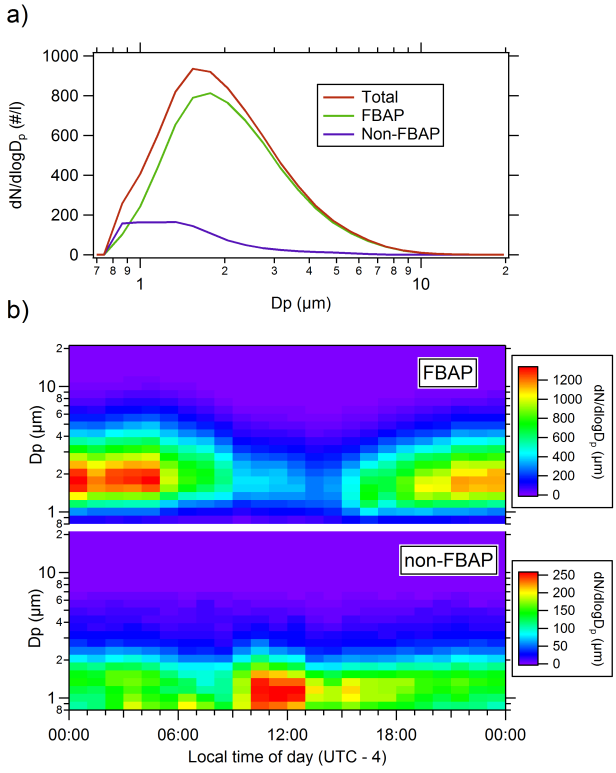

Figure 8. Particle number size distributions measured with the WIBS-3: a) mean size distributions for Total, FBAP and non-FBAP; and b) diurnal variation of size distribution for FBAP and non-FBAP (note that the colour scales are not the same).

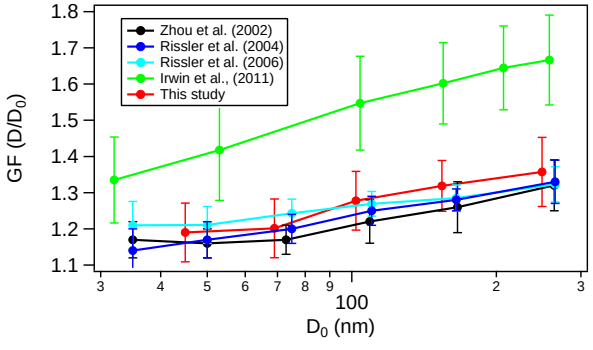

Figure 9. Mean growth factor for the dominant less hygroscopic mode plotted agains dry diameter, comparing this to previous studies in Amazonia and Borneo. The data from Rissler et al. (2004) and Rissler et al. (2006) represent "less" and "moderately hygroscopic" particles (respectively) during the wet season. Error bars represent ± 1 standard deviation.

Atmos. Chem. Phys. Discuss., doi:10.5194/acp-2015-1020, 2016
Manuscript under review for journal Atmos. Chem. Phys.
Published: 18 January 2016

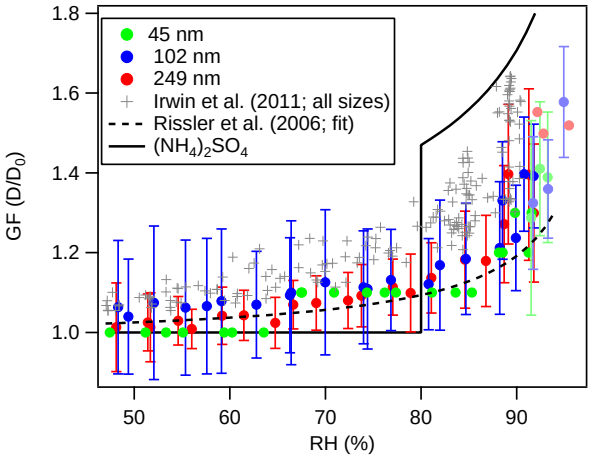

Figure 10. Humidogram (dependency of growth factor on RH), taken between 14:00 and 20:30 UTC on the 21st July. The fainter points at higher RH were taken between 13:30 and 14:30 UTC on the 23rd July. The humidogram data from Irwin et al. (2011), and the humidogram fit from Rissler et al. (2006) are also shown, for comparison. The black line shows the modelled humidogram for ammonium sulphate (Topping et al., 2005) for reference.

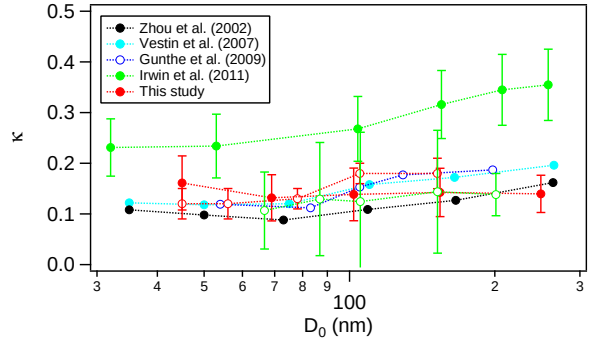

Figure 11. Comparing κ as a function of diameter for this and previous studies in Amazonia and Borneo. Filled circles represent HTDMA derived values, while empty circles are CCNc derived values. Error bars represent $\pm$ 1 standard deviation, where this data is available. The values for Zhou et al. (2002) and Vestin et al. (2007) were calculated by Gunthe et al. (2009).

Atmos. Chem. Phys. Discuss., doi:10.5194/acp-2015-1020, 2016
Manuscript under review for journal Atmos. Chem. Phys.
Published: 18 January 2016

Atmospheric Chemistry and Physics Discussions

Table 2. Mean derived parameters from CCNc measurements for each set supersaturation, along with ± standard deviation.

SS (%)	D_{50} (nm)	κ	N_{CCN} (cm^{-3})
0.15	152 ± 9.5	0.18 ± 0.03	87 ± 35
0.26	105 ± 5.5	0.18 ± 0.03	161 ± 60
0.47	78 ± 4.2	0.13 ± 0.02	212 ± 74
0.80	56 ± 3.0	0.12 ± 0.02	248 ± 82
1.13	45 ± 3.4	0.12 ± 0.03	268 ± 86

Table 3. Solutions to the Ward linkage cluster analysis, showing mean (± 1 standard deviation) intensity in each fluorescence channel (FL1 - 3), optical particle diameter (D_p) and assymmetry factor (A_f).

	Cl1	Cl2	Cl3
FL1 (280 nm)	1400 ± 302	478 ± 386	386 ± 533
FL2 (280 nm)	120 ± 96	33 ± 47	351 ± 212
FL3 (370 nm)	94 ± 106	47 ± 73	721 ± 379
D_p(µm)	2.5 ± 1.3	1.9 ± 1.0	2.3 ± 1.1
A_f	30.9 ± 15.0	30.2 ± 15.7	29.0 ± 15.1